RSC Advances

This article can be cited before page numbers have been issued, to do this please use: S. Andleeb, I. Imtiaz-ud-Din, M. K. Rauf, S. S. Azam, A. Badshah, H. Sadaf, A. Raheel, M. N. Tahir and S. Raza, *RSC Adv.*, 2016, DOI: 10.1039/C6RA19162B.

ROYAL SOCIETY OF CHEMISTRY

www.rsc.org/advances

View Article Online
DOI: 10.1039/C6RA19162B

A One-pot Multicomponent Facile Synthesis of Dihydropyrimidin-2(*1H*)-thione Derivatives using Triphenylgermane as a Catalyst and its Binding Pattern Validation

Received 00th January 20xx,
Accepted 00th January 20xx

DOI: 10.1039/x0xx00000x

www.rsc.org/

Sohaila Andleeb, [a] Imtiaz-ud-Din, [a] * Muhammad Khawar Rauf, [a] * Syed Sikander Azam, [c] Amin Badshah, [a] Haseeba Sadaf, [a] Ahmed Raheel, [a] Muhammad Nawaz Tahir, [b] Saad Raza, [c]

A series of substituted dihydropyrimidin-2(*1H*)-thione derivatives (**1**-**8**) have been synthesized by using a facile and modified procedure using triphenylgermyl propionate as a catalyst. On comparison with classical Biginelli reaction, this new protocol has the advantages of excellent yield and shorter reaction time. The synthesized compounds have been characterized by various spectroscopic techniques such as FT-IR, multinuclear ($^{1}H/^{13}C$) NMR spectroscopy and single crystal XRD analysis.The molecular docking studies was performed to identify the probable binding modes of potent inhibitors in the active site of the enzymes *Human topoisomerase II alpha* (4fm9) and *Helicobacter pylori urease* (1E9Y). Compound **3** was found to be the most potent inhibitor according to the molecular docking scores and molecular dynamic simulation which suggests they can further be processed as lead molecule to interpret the pharmacologic properties of these compounds.

Introduction

Thiones, in particular dihydropyrimidin-2(*1H*)-thiones have been reported to possess remarkable pharmacological applications such as antiviral, antibacterial, antihypertensive, anti-inflammatory, anticancer activity [1, 2] and can act as calcium channel modulators as well as multi- drug resistance reversal [3, 4] The ring system of pyrimidine, being present in many biomolecules such as vitamins and nucleic acids, play an important role in various biological processes [5]. Keeping in view these aspects, their synthesis has become the focus of great interest for organic and medicinal chemists [6]. Pietro Biginelli reported the acid catalysed cyclocondensation reaction of ethyl acetoacetate, benzaldehyde and urea [7], and the novel product (3,4-dihydropyrimidin-2(*1H*)-thione) was obtained by simply heating a mixture of the three components dissolved in ethanol with a catalytic amount of HCl at refluxing temperature. Unfortunately, the synthetic potential of this new heterocyclic compound remained unexplored for quite some time till the 1980s. Synthesis of many other heterocyclic scaffolds has also been attributed to these quite flexible precursors [8, 9]. One of the major drawbacks associated with Biginelli condensation is low products yield (30–35%). In recent years, several methods to improve the yield using triphenyl phosphine [10], $ZrCl_4$ [11], SiO_2/H_2SO_2 [12], granite [13], trichloroisocyanuric acid [14], copper(II) sulfamate [15], nafion-*H* [16], *p*-sulfonic acid calixarenes [17] and $[Al(H_2O)_6](BF_4)_3]$ [18] have been reported in the literature (Table 1). To overcome the problems associated with the reported methodologies there is a need for a simple and efficient method to synthesize dihydropyrimdin-2(*1H*)-thiones under mild conditions. Apart from the synthesis of organogermanium compounds, their new applications have also been explored [18-20]. A detailed literature survey clearly suggested that there is no report yet on the application of triphenylgermane as Lewis acid catalyst for the classic Biginelli and Hantzsch condensation reactions. Research work was further extended to develop a most plausible mechanism for the synthesis of dihydropyrimidines using Ph_3GeH as catalyst. We here are now able to propose a new reaction mechanism whereby organogermane in presence of catalytic amount of HCl (produced *in situ*) play an active role in the synthesis of dihydropyrimidin-2(*1H*)-thiones in excellent yield.

[a]*Department of Chemistry,Quaid-i-Azam University, Islamabad-45320, Pakistan, E-mail: drimtiazuddin@yahoo.com; Fax: +92 51 90642241; Tel: +92 51 9064210; mkhawarrauf@yahoo.co.uk; Fax: +92 51 90642241; Tel: +92 51 90642226*
[b]*Department of Physics, University of Sargodha, Sargodha, Pakistan.*
[c]*Computational Biology Lab, National Center for Bioinformatics, Quaid-i-Azam University, Islamabad-45320, Pakistan*

Electronic Supplementary Information (ESI) available: [CCDC nos. for **1**, **2**, **3**, **4** and **7** are 1419339, 1063506, 1419338, 1063500, and 1419340. For crystallographic data See DOI: 10.1039/x0xx00000x

View Article Online
DOI: 10.1039/C6RA19162B

In the recent years, sulfur containing compounds has shown remarkable medicinal applications due to their pharmacological and biological significance. Prior to the *in vitro* studies, we preferred to explore the protein binding capacity of these compounds by using *in silico* techniques against Human *topoisomerase II alpha* (PDB ID=4fm9) and *Helicobacter pylori urease* (PDB ID=1E9Y). The targets used are considered to be representative for anticancer and urease inhibition studies.

Results and discussion

Synthesis and Chemistry

The designed 3,4-dihydropyrimidin-2(*1H*)-thiones (**1**-**8**) were synthesized in a single step. Catalytic amount of triphenylgermyl propanoic acid was treated with $SOCl_2$ and excess of $SOCl_2$ was removed prior to dilution with acetone. Calculated quantity of KSCN was added and stirred for 30 minutes, and then a solution of substituted aniline was added. Aqueous workup in acidified chilled water affords dihydropyrimidin-2(*1H*)-thione (**1**-**8**) in excellent yields (Scheme 1).

Biginelli's reaction is quite sensitive to the choice of solvent, catalyst and the reactants, in particular, carbonyl compounds being used. Parallel studies evaluating the effect of Ph_3GeH on product yield and its isolation settled that use of catalytic amount of triphenylgermane/HCl enhances the yield averaging to be 92%. The advantages of this kinetically more facile methodology are the lesser reaction time and ease of isolation. The data as mentioned in Table-1 manifested that our synthetic methodology is one of the best, although there are reports showing about 98% yield [13, 17(c)] but there are also some synthetic approaches which yielded the product less than 65% [12].

Earlier reports clearly depicts that Iminium, Enamine and Knoevenagel mechanisms are the three main mechanistic approaches that are well established for the Biginelli's reaction and a kinetic model also suggests that a catalyst used in Biginelli reaction not only improves the yield of products and reduces the reaction time but also responsible for selection of reaction pathway, thereby favouring the possible mechanism involved [21]. Choice of triphenylgermane as a catalyst facilitates imminium mechanism which involves the reaction of substituted anilines and HSCN to produce thiourea intermediates **II**(**a**-**h**) followed by their reaction with methylpent-3-en-2-one (**I**) whose stereoselectivity has been tuned by hydrogermane used as catalyst.

Table 1. Comparative overview of the catalytic activity of various catalysts for the synthesis of Biginelli's type 3,4-dihydropyrimidin-2(*1H*)-thiones/ -ones [1, 10-17].

Catalyst/ Refs.[a]	Solvent/ Temp.[b]	Time (h)	Yield (%)
Triphenyl phosphine [10]	Solvent free/ 100^0C	10	70-80
$ZrCl_4$ [11]	C_2H_5OH/ reflux	6	80-88
Silica/H_2SO_4 [1]	C_2H_5OH/ reflux	6	85-90
Granite [12(a)]	C_2H_5OH/ reflux	3.5	60-65
$InBr_3$ [12(b)]	C2H5OH/ reflux	10	50-56
Trichloroisocyanuric acid [13]	C_2H_5OH/ reflux	12	85-90
Copper(II) sulfamate [14]	CH_3COOH/ 100^0C	6	75-80
Nafion-*H* [15]	C_2H_5OH/ reflux	5	75-90
p-Sulfonic acid calixarenes [16]	C_2H_5OH/ reflux	8	75-80
$[Al(H_2O)_6](BF_4)_3]$ [17(a)]	CH_3CN/ reflux	20	75-80
Yttria-Zirconia base Lewis acid [17(b)]	CH_3CN/ reflux	4-16	81-94
Metallo-phthalocyanines [17(c)]	CH_3CN/ reflux	5	82-98
$LaCl_3{\cdot}7H_2O$ [17(d)]	C_2H_5OH/ reflux	5	56-97
Phenylboronic acid [17(e)]	CH_3CN/ reflux	18	60-97
Ph_3GeH Present work	acetone/ reflux	3	90-96

[a] References [b] Temperature

The overall reaction, involving the formation of 4-methylpent-3-en-2-one (**I**) and thioureas **II**(**a**-**h**) with the use of substituted anilines instead of aldehydes as mentioned in Biginelli's reaction, to produce

View Article Online
DOI: 10.1039/C6RA19162B

dihydropyrimidin-2(*1H*)-thiones (**1**-**8**), has been shown in Scheme 2. Triphenylgermylpropanoic acid produces HCl on reaction with $SOCl_2$ as shown in scheme 2 that leads to a pathway study suggesting the formation of 4-methylpent-3-en-2-one (**I**), produced by acid-catalyzed aldol reaction between two ketonic molecules as depicted in scheme 2. Formation methylpent-3-en-2-one in step 1 has been reported [22].

Scheme 1. Synthesis of dihydropyrimidin-2(*1H*)-thiones (**1**-**8**).

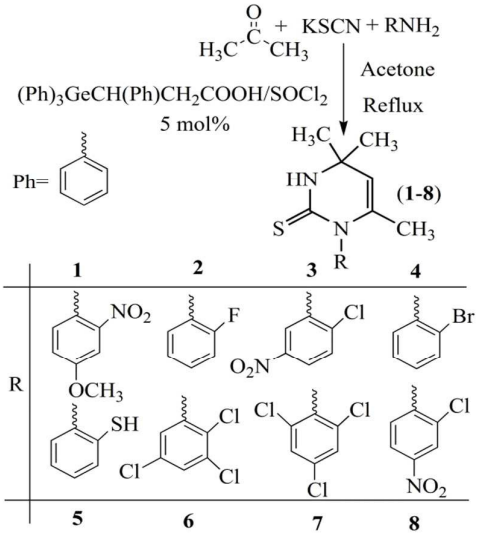

Scheme 2. Plausible mechanism for (**1**-**8**).

Step-I: Acid halide formation.

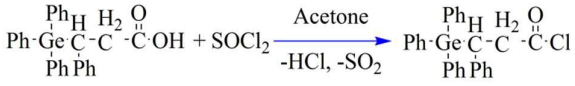

Step-II: Catalyzed conversion of acetone to 4-methylpent-3-en-2-one (**I**).

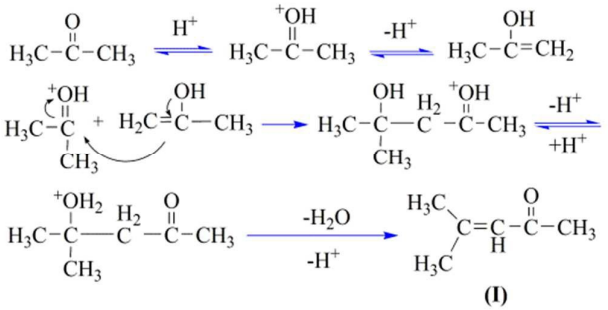

Step-III: Formation of thiourea species II (a-h)

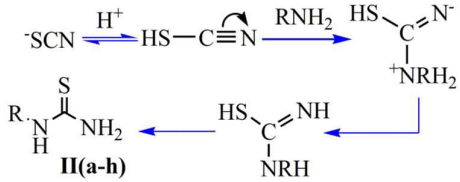

Step-IV: Organogermane catalyzed reaction between (**I**) and (**II**).

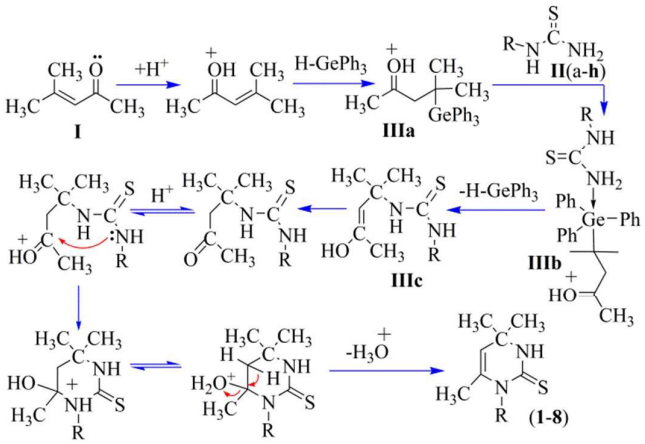

The overall reaction can be delineated as follows;

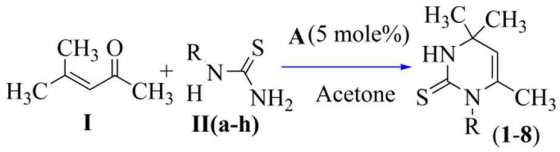

Formation of acid catalyzed acyl imine intermediate as a key rate determining step in Biginelli reaction has been proposed and established by Kappe [8]. Formation of methylpent-3-en-2-one (**I**) in scheme 2 (step **I**) proceeds with hyrometallation where triphenylgemanium hydride adds to **I** following Anti Markovnikov addition. Owing to expandable *d*-orbital of germanium, an intermediate **IIIb** forms between **IIIa** and **II**(**a**-**h**) through a coordinate bond following associative mechanism which is not stable enough and triphenylgemanium leaves as triphenylgemanium hydride through dissociative mechanism forming $\mathbf{III_c}$. A keto-enol tautomerisim establishes in the subsequent step which under acidic conditions favors enol form. As earlier reports suggest, the presence of HCl activates the enol form whose quantity accounts for all the facets of Lewis aid catalyzed Biginelli reaction [23]. This enol form undergo cyclocondensation forming 3, 4-

View Article Online
DOI: 10.1039/C6RA19162B

dihydropyrimidin-2(*1H*)-thiones (**1**-**8**) as shown in scheme 2 (step-IV).

It is important to mention that wider functional group tolerance is exhibited here by hydrogermalylation as compared to that displayed in previously known Lewis acid catalyzed methodologies [24]. Indeed due to lower oxophilicity of germanium as compare to silicon, chemoselectivity of the reaction is affected, giving much more clean and high yielding product without disturbing the alkoxy substituents present on the aniline used, even if excess of the germane is used.

Triphenylgermylpropanoic acid readily produces organogermane species on decomposition as evident from the mass spectral studies of our earlier reports [25, 26]. The oxidation potential of triphenyl germane, as measured by cyclic voltammetry, is +0.94V, which conforms to its easy oxidation leading to triphenylgermyl species. Moreover, the intermediacy of this oxidatively generated triphenylgermyl radical has also been proven using spin trapping experiments with phenyl *t*-butyl nitrone [27]. These organogermanium hydrides have been used as transition-metal-catalyzed hydrogermylation of alkenes and alkynes since mid-1950s [28]. Since the initial report of Gilman [29], limited reports have been published on radical hydrogermylation of π-systems [27]. Besides the radical mechanistic framework, transition-metal-catalyzed hydrogermylation of terminal alkynes has been more extensively studied with catalysts based on rhodium [30], palladium [31], ruthenium [32] and iron [33]. Two last classes of hydrogermylation that support our concept of hydrogermylation of 4-methylpent-3-en-2-one (**I**), as enunciated in Scheme 2, is the Gevorgyan Lewis acid catalysed hydrogermylation of terminal alkynes and the Schweizer's stereoselective hydrogermylation of α-trifluoromethylated alkynes [34]**.** As an attempt to discover a plausible route to meet the challenge of high yield synthesis of dihydropyrimidine thiones, we envisioned that a hydrogermylation reaction, whose stereoselectivity has been tuned under the present set of catalytic acidic conditions, could potentially provide an efficient and divergent route to substrate (**I**) that could be further used in cross-coupling reactions after germanium electronic tuning. Finally this tuning of the electron deficiency of the germanium atom makes cross coupling of **II**(**a**-**h**) facile which further on losing water molecule produces the target compounds (**1**-**8**). Catalytic role of organogermane, produced *in situ*, was further confirmed by repeating the same methodology using acylation of *trans*-3-phenyl-2-propenoic acid where no Ph_3GeH moiety is present in the acid that results in a mixture of products containing low yield of dihydropyrimidine thiones. When this study was undertaken in the presence of organogermanium, there is a tremendous improvement in the yield as well as the product isolation becomes facile. This study was further continued by decreasing the amount of triphenylgermyl propanoic acid to different mole ratios and it was determined that the catalytic system works efficiently up to 5 mole%.

Spectroscopic Studies

The spectroscopic data, mentioned in the experimental section, fully characterized the formation of target compounds. Tentative assignments of peaks in the FT-IR spectra of the compounds (**1**-**8**) have been made on the basis of earlier publications [35, 36]. The infrared spectra show five absorption bands of interest namely ν(N-H), ν(C-H)Ar, $\nu(C\text{-}H)_{aliphatic.}$, ν(C=C) and ν(C=S) at 3231-3185, 3032-2944, 2883-2850, 1560-1515 which range from weak to strong intensities respectively. Many other prominent peaks like C-F, C-Cl, SH and NO_2 have also been observed in their respective regions.

The ^{1}H NMR data demonstrate that all the protons show characteristic chemical shift values in their respective regions identified by their intensity and multiplicity pattern and the total number of protons calculated from the integration curve is in agreement with the presented molecular composition. The NH protons in all the synthesized compounds appeared as broad peak near 7 ppm while a quartet around 4.81-5.04 ppm shows the splitting of methylene proton by neighbouring methyl protons on vicinal carbon. Two methyl substituents at carbon next to thiourea NH show two singlets at different chemical shifts due to magnetic non-equivalence. Three protons of methyl substituent at carbon next to the methylene carbon

View Article Online
DOI: 10.1039/C6RA19162B

show doublet in range of 1.43-2.55 ppm while protons in the aromatic region are sensitive towards the substituent attached to phenyl ring and change their positions and multiplicities accordingly. In compound **1** proton attached to carbon in vicinity of nitro group shows a splitting into a doublet due to coupling with three methyl protons in its close vicinity. Due to higher electron withdrawing effect of NO_2 groups this proton (-C=CNO_2) is highly deshielded and a higher downfield shift at 7.58-7.59 ppm is observed. Methoxy protons give a clear singlet at 3.92 ppm. In compound **2**, **4** and **5** proton attached at carbon adjacent to F, Br and S shown higher downfield shift and their chemical shift values are slightly higher than other protons of phenyl ring. In compound **3** a doublet is observed for proton at carbon next to nitro group (=C-CNO_2) around 8.28ppm while the proton at carbon next to nitro group (-C=CNO_2) shows multiplet instead of singlet due to coupling with methyl protons as for compound **1**. A singlet at 3.4ppm in compound **5** indicates the presence of SH proton.

The ^{13}C NMR data show that signals found correspond with the presence of magnetically non-equivalent carbon atoms, assigned by comparison of the experimental chemical shift values with those calculated from the incremental method [37]. Highly deshielded carbon in ^{13}C NMR spectra of target compounds (**1**-**8**) at 177.7-176.6ppm indicate the presence of C=S functionality. The phenyl ring carbons containing strong electron withdrawing groups e.g., NO_2, F, Cl, Br resonate at low field while carbon of methyl substituent appear up field.

Crystallographic discussion (1-4, 7)

Crystallographically suitable single crystals of (**1**-**4**, **7**) for X-ray analysis were grown from dichloromethane solution by slow evaporation at room temperature. The ORTEP structures of dihydropyrimidin-2(*1H*)-thione (**1**-**4**, **7**) along with numbering schemes are illustrated in Fig. 1 and the selected geometric parameters are presented in Supplementary Table 2. The dihydropyrimidin-2(*1H*)-thiones moiety is nearly planar in all the molecules as evident from the associated torsional angles. The reason for this planarity, however, can be accredited to the delocalization of π-electron density over the thiourea moiety, which is evidenced by the shorter N–C bond lengths [1.317–1.479 Å] listed in Supplementary Table 2, and hence the shortest N-C bond lengths [1.317-1.326Å] confirm the partial double bond character of N-C in (H)N–C=S moiety due to C=S/SH tautomerism.

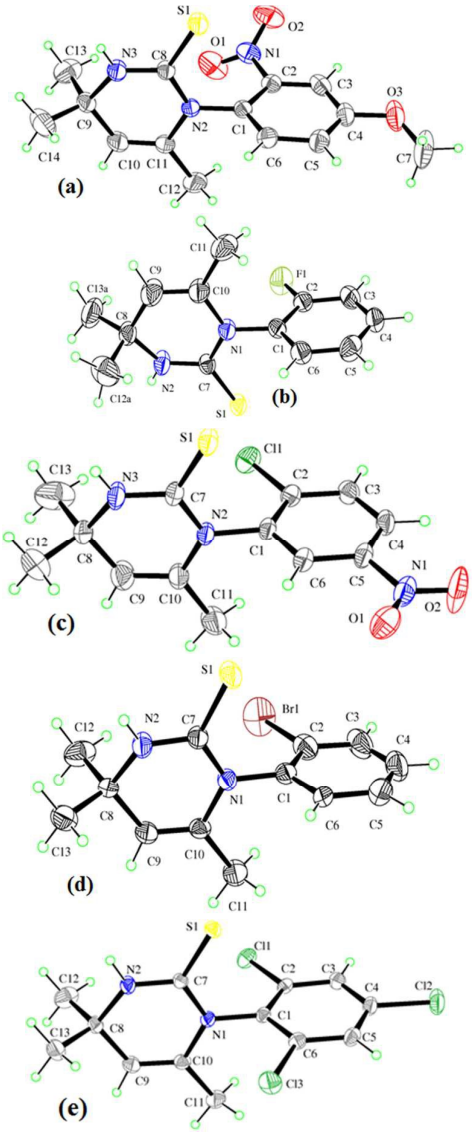

Fig. 1 ORTEP view showing 35% probability ellipsoids (**a**-**e**) of (**1**-**4**, **7**) with atom numbering scheme.

The longer N-C bond lengths [1.452–1.472 Å] (**1**-**4**, **7**) and [1.470-1.479Å] (**1**, **3**) observed for HN-Csp^3 and O_2N-Csp^2 respectively. These elongations in N-C bond lengths can be associated with the lesser *s* character of C$sp^3$and the electron withdrawing effect of –NO_2group.

View Article Online
DOI: 10.1039/C6RA19162B

The molecular structure of **1** {Figure **2(f)**} shows intermolecular N(3)-H(3A)···S(1) 2.500Å and C(12)-H(12A)···O(2) 2.699Å hydrogen bonds stabilizing the thiones geometry mainly due to the centrosymmetric dimers $\{\cdots H\text{-}N\text{-}C{=}S\}_2$ connected by N–H···S^{i} (2.500Å) ((i) −x+1, −y+2, −z+1) as well as by comparatively weak C–H···O (2.699Å) hydrogen bonds.

In the crystal packing of **2** {Figure **2(g)**}S atom (C=S) shows trifurcated intermolecular N(2)-H(2)···S(1)^{i} 2.638Å, C(5)-H(5)···S(1) 2.920Åand C(6)-H(6)···S(1)^{ii} 2.975Å ((ii) −*x*, −*y*+1, −*z*+1) hydrogen bonds stabilizing the thiones geometry. These molecular structures also fashioned the centrosymmetric dimers $\{\cdots H\text{-}N\text{-}C{=}S\}_2$ connected by N–H···S^{i} (2.638Å) {(i) −*x*, −*y*, −*z*+1}. Similar type of intermolecular interactions has also been observed for **4** {Figure **2(i)**}.

In the crystal packing of **3**, the sulphur atom (C=S) involved in the formation of synthones $\{\cdots H\text{-}N\text{-}C{=}S\}_2$ is bifurcated {Figure **2(h)**} forming N(3)-H(3A)···S(1)^{i} 2.559Å {(i) −*x*+1, −*y*, −*z*)} hydrogen bonds and additional C(7)-S(1)···Cl(1) 3.493Å interactions. The weak intermolecular molecular interactions C(11)-H(11C)···O(1) 2.392Å {(ii) *x*−1, *y*, *z* } and N(1)-O(1)···O(1) 2.970Å have also been observed to stabilizing the crystal packing in **3**. Similar to the crystal packing of **3**,sulfur atoms (C=S) in **7**also involved in the formation of dimeric synthones $\{\cdots H\text{-}N\text{-}C{=}S\}_2$through N(2)-H(2A)···S(1)^{i}2.593Å {(i) −*x*+1, −*y*+1, −*z*+1} hydrogen bonds is bifurcated {Figure **2(j)**} forming additional C(5)-H(5)···S(1) 2.873Å {(ii) −*x*+1, *y*−1/2, −*z*+1/2} interactions {Supplementary Table 3}. Molecular structures of **4** and **7** additionally show C-H···Br and C-H···Cl hydrogen bonds stabilizing their geometry, respectively. The dihedral angles between the aromatic rings C(1)-C(6) and dihydropyrimidin-2(*1H*)-thione moieties for **1**-**4** and **7** are 86.06, 85.85, 88.66, 84.23 and 85.69˚, respectively. The narrow variation in dihedral angles subtended by aromatic rings with dihydropyrimidin-2(*1H*)-thione moieties through C-N bond reveal that the substituents have minimal effect on the conformational geometry of these molecules.

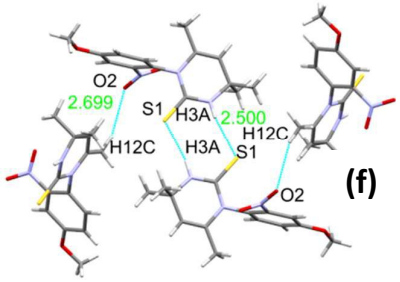

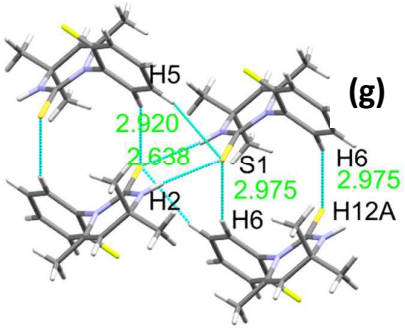

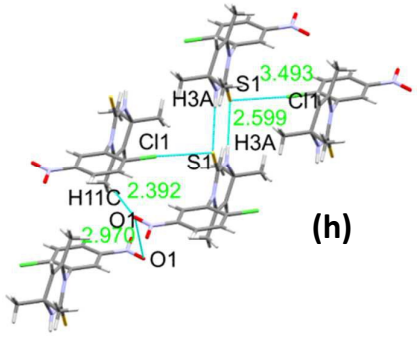

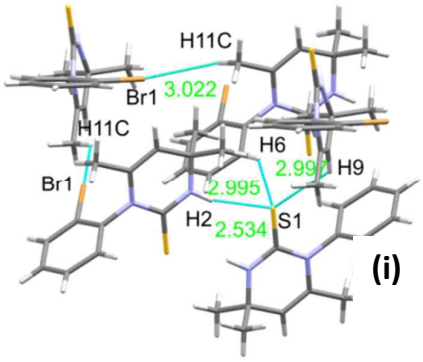

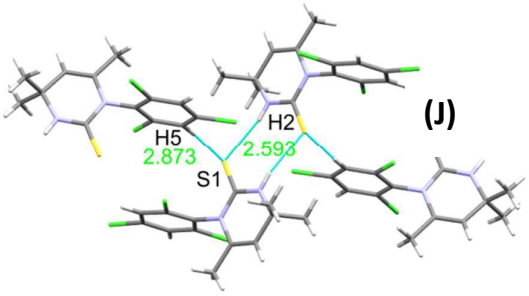

View Article Online
DOI: 10.1039/C6RA19162B

Fig. 2 View on the hydrogen bonded 1D structures (**f**-**j**) for (**1**-**4**, **7**).

Molecular Docking

Molecular Docking Studies of Human topoisomerase II alpha

The docking results indicate that the inhibitor docked around Met762 (residue of active site) showed acceptable GoldScore (55.39) and acceptable binding energy values. VMD [38] and ligplot [39] analysis was performed in order to validate the in-depth interaction patterns between inhibitor and active site of 4fm9 (Supplementary Fig. 1-3). Studied compounds are involved in making conventional hydrogen bonds, hydrophobic interactions with the residues of active site region and salt bridge as well **8**.

Binding mode analysis

The docked complex is showing appreciable interactions of the active site residues as shown in the Fig 3. Active site residues inside 10 Å regions are involved in the stability of the compound inside the active site pocket.

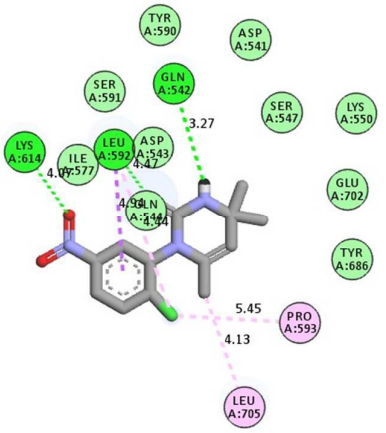

Fig.3.Interaction diagram of **3** with 4fm9

Molecular Docking Studies of Helicobacter pylori Urease

The docking results indicate that the inhibitor docked around active site (residue of active site) showed acceptable Gold Score 55.39. VMD [38] and ligplot [39] analysis was performed in order to validate the in-depth interaction patterns between inhibitor and active site of 1E9Y (Supplementary Fig.4-7). Studied compounds are involved in making conventional hydrogen bonds, hydrophobic interactions with the residues of active site region. The docking results indicate that the inhibitor docked around His322 (residue of active site) showed acceptable binding energy values (Table 2).

Binding mode analysis

The docked complex is showing appreciable interactions with the active site residues as shown in the Fig. 4. Vander-Waals and hydrogen bonding is also involved in the stability of the compound used in the active site pocket.

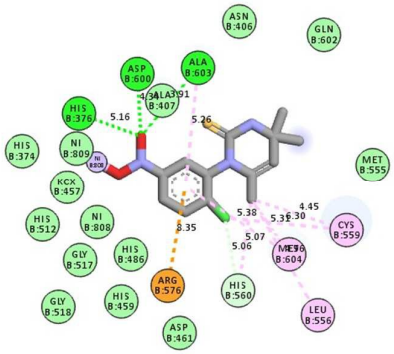

Fig. 4.Interaction diagram of **3** with 1e9y

Molecular Dynamics of complexes

Docked compound **3** with Human topoisomerase II alpha and Helicobacter pylori urease were simulated in a molecular environment to establish their significance against these targets. Top scored compound **3** was selected among the derivatives (**1**-**8**) to sum up their behaviour, and we are looking for the best candidates among these derivatives to be used as potential lead. Initial docked conformation showed promising binding with the active site for 1EY9 and 4FM9 but to further establish their binding pattern and to give some baseline for their mechanism against these enzymes, molecular dynamics simulation was carried out on these docked complexes. The residue numbers are restarted from 1 by simulation package, if there is no structural information of those residues in pdb file. So, there is a difference in number of residues in pdb and simulation trajectory of 4FM9 which is 432. During the

View Article Online
DOI: 10.1039/C6RA19162B

simulation the average mean deviation in backbone of 1E9Y is observed as 2.02 Å (Figure 5a) and

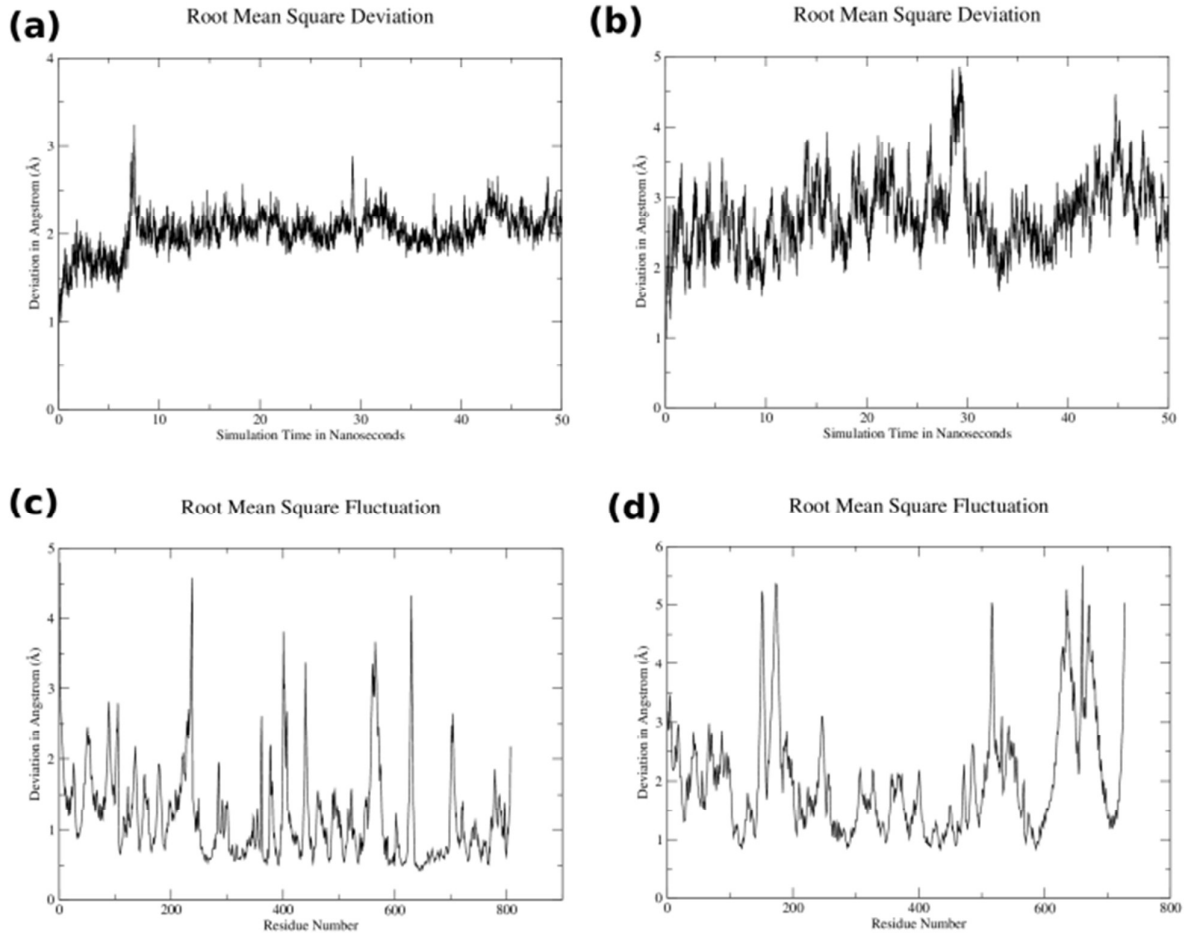

Fig. 5 Root mean square deviation (a) and (b) of backbone of complex of compound **3** with 1E9Y and 4FM9 respectively, and root mean square fluctuation (c) and (d) of residues for the trajectories of 1E9Y and 4FM9 respectively during the course simulation.

Table 2. Docking scores

No.	Human topoisomerase II alpha (*4FM9*)		Helicobacter pylori Urease (*1E9Y*)	
	Binding Energy	**Gold score**	**Binding Energy**	**Gold score**
1	-6.0	50.10	-6.8	51.85
2	-8.1	46.16	-7.2	45.10
3	-7.3	55.39	-7.6	57.72
4	-7.3	49.06	-7.1	46.50
5	-6.9	49.27	-6.9	48.75
6	-7.0	52.23	-6.5	50.52
7	-7.3	50.42	-6.0	48.09
8	-7.2	50.72	-6.5	57.07

We see a relatively larger deviation of 2.74 Å in 4FM9 (Figure 5b). According to the root mean square deviation (RMSD) and root mean square fluctuation (RMSF) value you can see that the 1EY9 is relatively

View Article Online
DOI: 10.1039/C6RA19162B

more stable than the 4FM9 (Figure 5c). The main cause of this deviation is the two large helices which make up the unique folds of 4FM9. These helices are present from residue number 600 and onwards in the protein 4FM9 which are clearly visible in RMSF graph of 4FM9 showing higher rate of fluctuation then the rest of protein (Figure 5d). Overall the 4FM9 is having higher fluctuations than 1E9Y, button the other hand the compound **3** is found to be in the vicinity of initial docked site of 4FM9 throughout the simulation time frame. The snapshots taken at different intervals suggest that the compound **3** stays near the residue GLN 110 and ASP 111. Initially the compound is found to be actively interacting via hydrogen bonds to polar residue around it (Figure 6a). As the simulation proceed for 20 nanoseconds (ns) we can see that some of the interacting partners are lost but it firmly attaches itself to the backbone of GLN110 and ASP111 (Figure 6b).

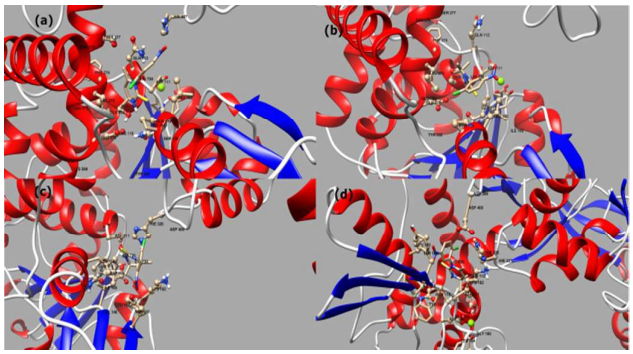

Fig. 6 Snapshot taken at intervals of (a) 1 ns, (b) 20 ns (c) 40 ns and (d) 50 ns from the simulation trajectory of complex of compound **3** with 4FM9.

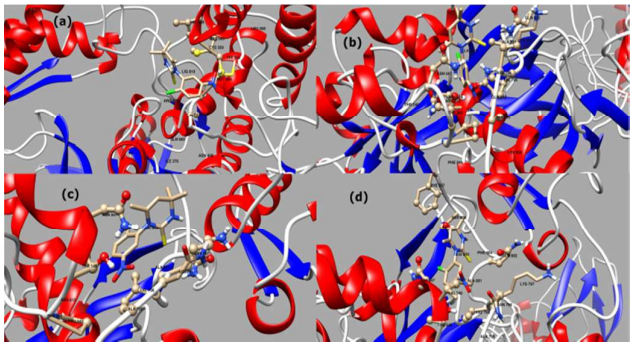

Fig. 7 Orientation of compound **3** around 1E9Y at simulation time intervals of (a) 1ns, (b) 30 ns, (c) 40 ns and (d) 50 ns.

After another 20 ns we can see it acquires new polar residue around it (Figure 6c). For the last 10 ns we can see that these partners slight vary but the compound does not leave its initial position (Figure 6d). In case of 1E9Y the compound 3 drifts away from initial site but after 30 ns it chooses another site to interact and binds slightly away from its initial position (Figure 7a). From the snapshots taken after 30 ns the compound **3** appears to have bonded to this site for the rest of 20 ns of simulation. From the snapshot taken at 30 ns compound **3** has adjusted itself around polar residue ASN 547, THR 545, ASN 796, LYS 797 and GLN 802 (Figure 7b). These interacting partners of continue to exist around the compound **3** after 20 ns, which are seen in a snapshot taken at 40 ns (Figure 7c) and 50 ns (Figure 7d). This behaviour of compound **3** in the presence of enzymes 1E9Y and 4FM9 could suggest that it can actively suppress the human topoisomerase II alpha and it can indirectly or directly alter the activity of *Helicobacter pylori* urease.

Experimental

Chemicals/instrumentation

All reagents and solvents used in this study were obtained from the supplier and recrystallized/ redistilled as required. (*E*)-3-phenylprop-2-enoic acid was purchased from Sigma Aldrich (Germany), while procuration of germanium dioxide (99.9% purity) was made from the People's Republic of China and was used as received. 3-triphenylgermyl-3-phenylpropanoic acid was prepared according to reported methods [18, 20].Thin layer chromatography (TLC) was performed using aluminium sheets coated with silica gel 60 F254 (Merck). Melting points of all the synthesized compounds have been determined in open capillary tubes by using a Gallenkamp apparatus (MP-D) and were uncorrected. IR spectra in the range of 4000–400 cm^{-1} were obtained on a Thermo Nicolet-6700 FT-IR Spectrophotometer. The ^{1}H and ^{13}C NMR spectra were recorded on a Bruker spectrometer at 300 MHz and 75 MHz in $CDCl_3$, respectively using residual solvent signals as a reference.

Synthesis of dihydropyrimidin-2(*1H*)-thiones(1-8)

View Article Online
DOI: 10.1039/C6RA19162B

The general procedure used for the synthesis of target compounds (**1**-**8**) is as follows. About 1 ml $SOCl_2$ was added to 0.09 g (0.2 mmol) of 3-triphenylgermyl-3-phenylpropanoic acid (5 mol %) and stirred for two hours at 80˚C. Potassium thiocyanate 0.35 g (4.0 mmol) in dry acetone (30 ml) was then added drop wise and the solution was refluxed for 5-10 minutes and cooled. Afterwards 4.0 mmol of the respective substituted aniline was added and reaction mixture was stirred for an additional one hour. Progress of reaction was monitored using TLC. The reaction mixture was poured in a beaker containing crushed ice and stirred well. The solidified product was isolated and dried. Pure product was obtained by solvent extraction technique using chloroform/water mixture (thrice). Organic layer was collected and dried over $MgSO_4$, and left for crystallization to obtain the target compounds (**1**-**8**).

Spectroscopic data for (1-8)

1-(4-Methoxy-2-nitrophenyl)-4,4,6-trimethyl-3,4-dihydropyrimidine-2(1H)-thione (**1**)

Generalized procedure described above was used for synthesis of 1 using 0.65 g (4.0 mmol) of 2-nitro-5-methoxyaniline to produce a pale yellow crystalline solid (yield; 96%): m.p. 220-222 ^{o}C; FTIR (cm^{-1}): 3211 (N-H), 3020 (C-$H_{aromatic}$), 2876 (C-$H_{aliphatic}$), 1552 (C=S). ^{1}H NMR (300 MHz, $CDCl_3$, ppm) δ: 7.59-7.58 (d, 1H, *J* = 3 Hz, ArH), 7.33-7.27 (m, 1H, ArH), 7.20-7.19 (d, 1H, *J* = 3 Hz, ArH), 7.01 (s, 1H, -NH-), 4.88-4.89 (m, 1H, -CH), 3.92 (s, 3H, -OCH_3), 1.57(s, 3H, -CH_3), 1.43(s, 3H, -CH_3), 1.37(s, 3H, -CH_3). ^{13}CNMR(75 MHz, $CDCl_3$) δ: 177.0, 159.6, 147.5, 141.4, 133.7, 131.6, 127.6, 119.5, 109.8, 56.0, 52.8, 31.9, 31.5, 20.3. Anal. calc. for $C_{14}H_{17}N_3O_3S$ (307.37): C, 54.71; H, 5.57; N, 13.67; S, 10.43. Found: C, 54.65; H, 5.56; N, 13.75; S, 10.41.

1-(2-Fluorophenyl)-4,4,6-trimethyl-3,4-dihydropyrimidine-2(1H)-thione **(2)**

The methodology used for the synthesis of **2** is the same as used for **1** using 0.44 g (4.0 mmol) of 2-fluoroaniline to produce pale yellow crystalline solid (yield; 90%): m. p. 192-194 ^{o}C; FTIR (cm^{-1}): 3196 (N-H), 2963 (C-$H_{aromatic}$), 2852 (C-$H_{aliphatic}$), 1521(C=S); ^{1}H NMR (300 MHz, $CDCl_3$, ppm) δ: 7.42-7.14 (m, 4H, ArH), 6.99 (s, 1H, -NH), 4.87-4.86 (m, 1H, -CH), 1.56 (s, 3H, -CH_3), 1.40-1.37 (m, 6H, -CH_3); ^{13}C NMR (75 MHz, $CDCl_3$) δ: 177.7 (C=S), 133.9, 131.9, 130.4, 128.5, 124.2, 124.1, 116.1, 109.6, 52.5, 31.3, 31.2, 19.9. Anal. calc. for $C_{13}H_{15}FN_2S$ (250.34): C, 62.37; H, 6.04; N, 11.19; S, 12.81. Found: C, 62.32; H, 6.00; N, 11.24; S, 12.79.

1-(2-Chloro-5-nitrophenyl)-4,4,6-trimethyl-3,4-dihydropyrimidine-2(1H)-thione **(3)**

The methodology used for the synthesis of **3** is the same as used for **1** using 0.70 g (4.0 mmol) of 2-chloro-5-nitroaniline to produce a pale yellow crystalline solid (yield; 90%) m.p.199-201^{o}C; FTIR (cm^{-1}): 3207 (N-H), 3013 (C-$H_{aromatic}$), 2873 (C-$H_{aliphatic}$), 1547 (C=S); ^{1}H NMR (300 MHz, $CDCl_3$, ppm) δ: 8.28-8.20 (m, 2H, ArH), 7.68-7.64 (d, 1H, *J* = 9 Hz, ArH), 7.36 (s, 1H, -NH), 4.92-4.91 (m, 1H, -CH), 1.54 (s, 3H, -CH_3), 1.43 (s, 3H, -CH_3), 1.41 (s, 1H, -CH_3); ^{13}C NMR (75 MHz, $CDCl_3$, ppm) δ: 176.5 (C=S), 146.5, 141.6, 140.1, 139.5, 130.5, 127.6, 124.4, 110.2, 52.9, 31.7, 31.2, 20.0. Anal. calc. for $C_{13}H_{14}ClN_3O_2S$ (311.79): C, 50.08; H, 4.53; N, 13.48; S, 10.28. Found: C, 50.01; H, 4.51; N, 13.51; S, 10.30.

1-(2-Bromophenyl)-4,4,6-trimethyl-3,4-dihydropyrimidine-2(1H)-thione **(4)**

The methodology used for the synthesis of **4** is the same as used for **1** using 0.68 g (4.0 mmol) of 2-bromoaniline to produce a pale yellow crystalline solid (yield; 90%) m.p. 170-172 ^{o}C; FTIR (cm^{-1}): 3190 (N-H), 2954 (C-$H_{aromatic}$), 2851 (C-$H_{aliphatic}$), 1517 (C=S), ^{1}H NMR (300 MHz, $CDCl_3$) δ: 7.65 (d, 1H, *J* = 7.8 Hz, ArH), 7.46 (s, 1H, -NH), 7.39-7.37 (m, 1H, ArH), 7.29-7.19 (m, 2H, ArH), 4.85-4.84 (m, 1H, -CH), 1.49 (d, 3H, -CH_3), 1.44 (s, 3H, -CH_3), 1.37 (s, 3H, -CH_3); ^{13}C NMR(75 MHz, $CDCl_3$, ppm) δ 176.6 (C=S), 140.0, 133.0, 132.3, 131.3, 129.8, 127.8, 124.9, 109.6, 52.7, 32.0, 31.3, 20.2. Anal. calc. for $C_{13}H_{14}ClN_3O_2S$ (311.24): C, 50.17; H, 4.86; N, 9.00; S, 10.30. Found: C, 50.16; H, 4.85; N, 9.06; S, 10.27.

1-(2-Mercaptophenyl)-4,4,6-trimethyl-3,4-dihydropyrimidine-2(1H)-thione **(5)**

The methodology used for the synthesis of **5** is the same as used for **1** using 0.5 g (4.0 mmol) of 2-aminothiophenol to produce a pale yellow crystalline solid (yield; 90%) m.p. 168-170 ^{o}C; FTIR (cm^{-1}): 3185 (N-H), 2944 (C-$H_{aromatic}$), 2850 (C-$H_{aliphatic}$), 1515 (C=S); ^{1}H NMR (300 MHz, $CDCl_3$, ppm) δ: 7.67 (d, 1H, *J* = 6 Hz, ArH), 7.54-7.52 (d, 1H, *J* = 6 Hz, ArH), 7.44 (s, 1H, -NH), 7.41-7.38 (m, 1H, ArH), 7.31-7.26 (t, 1H, *J* = *9* Hz), 7.07

View Article Online
DOI: 10.1039/C6RA19162B

(s, 1H), 5.0 (s, 1H, -SH), 4.84-4.81 (m, 1H, -CH), 3.30-3.28 (d, 1H, *J* = 6 Hz), 1.47 (d, 3H, *J* = 3 Hz, -CH_3), 1.45 (s, 3H, -CH_3), 1.40 (s, 3H, -CH_3); ^{13}CNMR (75 MHz, $CDCl_3$) δ: 177.1(C=S), 139.2, 134.0, 133.8, 129.1, 128.9, 128.5, 126.5, 109.6, 49.6, 32.4, 31.1, 20.0. Anal. calc. for $C_{13}H_{16}N_2S_2$ (264.41): C, 59.05; H, 6.10; N, 10.59; S, 24.25 Found: C, 58.98; H, 6.08; N, 10.61; S, 24.22.

1-(2,3,5-Trichlorophenyl)-4,4,6-trimethyl-3,4-dihydropyrimidine-2(1H)-thione **(6)**

The methodology used for the synthesis of **6** is the same as used for **1** using 0.75 g (4.0 mmol) of 2,3,5-trichloroaniline to produce a pale yellow crystalline solid (yield; 92%) m.p. 230-231°C; FTIR (cm^{-1}): 3231 (N-H), 3032 (C-$H_{aromatic}$), 2883 (C-$H_{aliphatic}$), 1560 (C=S). ^{1}H NMR (300 MHz, $CDCl_3$, ppm) δ, 8.35 (s, 1H), 8.04-8.01(m, 1H), 7.01 (s,1H, -NH), 5.04-5.03 (m, 1H, -CH), 2.55-2.54 (d, 3H, *J* = 3 Hz), 2.34 (s, 3H, -CH_3), 2.31 (s, 3H, -CH_3); ^{13}C NMR (75 MHz, $CDCl_3$) δ: 179.0, 140.0, 139.3, 135.6, 138.8, 131.0, 130.0, 129.8, 110.0, 54.1, 36.2, 35.3, 22.1. Anal. calc. for $C_{13}H_{13}Cl_3N_2S$ (335.68): C, 46.51; H, 3.90; N, 8.35; S, 9.55. Found: C, 46.46; H, 3.89; N, 8.37; S, 9.56.

1-(2,4,6-Trichlorophenyl)-4,4,6-trimethyl-3,4-dihydropyrimidine-2(1H)-thione **(7)**

The methodology used for the synthesis of **7** is the same as used for **1** using 0.75 g (4.0 mmol) of 2, 4, 6-trichloroaniline to produce a pale yellow crystalline solid(yield; 92%) m.p. 237-238°C; FTIR (cm^{-1}): 3231 (N-H), 3032 (C-$H_{aromatic}$), 2883 (C-$H_{aliphatic}$), 1560 (C=S). ^{1}H NMR (300 MHz, $CDCl_3$, ppm) δ 8.35 (s, 2H, ArH), 7.08 (s, 1H, -NH), 5.04-5.03 (m, 1H, -CH), 2.55-2.54 (d, 3H, *J=3* Hz, -CH_3), 2.34 (s, 3H, -CH_3), 2.31 (s, 3H, -CH_3)); ^{13}C NMR (75 MHz, $CDCl_3$) δ: 178.5, 141.2, 138.9, 137.8, 132.0, 128.8, 111.0, 53.0, 36.1, 35.9, 23.6. Anal. calc. for $C_{13}H_{13}Cl_3N_2S$ (335.68): C, 46.51; H, 3.90; N, 8.35; S, 9.55. Found: C, 46.44; H, 3.88; N, 8.39; S, 9.53.

1-(2-Chloro-4-nitrophenyl)-4,4,6-trimethyl-3,4-dihydropyrimidine-2(1H)-thione **(8)**

The methodology used for the synthesis of **8** is the same as used for **1** using 0.70 g (4.0 mmol) of 2-chloro-4-nitroaniline to produce a pale yellow crystalline solid (yield; 90%) m.p. 201-203°C: FTIR (cm^{-1}): 3219 (N-H), 3022 (C-$H_{aromatic}$), 2880 (C-$H_{aliphatic}$), 1554 (C=S); ^{1}H NMR (300 MHz, $CDCl_3$, ppm) δ 8.96 (s, 1H, ArH), 8.23 (d, 1H, *J* = 6Hz, ArH), 7.68 (d, 1H, *J* = 6 Hz, ArH), 7.08 (s, 1H, -NH), 4.93-4.92 (m, 1H, -CH), 1.55-1.54 (d, 3H, *J* = 3 Hz, -CH_3), 1.45 (s, 3H, -CH_3), 1.42 (s, 3H, -CH_3); ^{13}C NMR(75 MHz, $CDCl_3$) δ: 176.5, 146.6, 141.9, 141.1, 139.5, 130.6, 128.0, 125.4, 110.2, 52.8, 31.6, 31.3, 20.0. Anal. calc. for $C_{13}H_{14}ClN_3O_2S$ (311.79): C, 50.08; H, 4.53; N, 13.48; S, 10.28. Found: C, 50.02; H, 4.50; N, 13.50; S, 10.46.

Crystallographic data collection and structural refinement

Single crystals of (**1**-**4**, **7**) were mounted on a thin glass fiber at room temperature and the reflection data were collected on a Bruker Kappa APE XII CCD diffractometer equipped with graphite mono-chromated MoKα radiation (λ= 0.71073 Å). The data were also corrected to Lorentz and polarization effect. The structure was solved using *SHELXS-97*. Final refinement on F^2 was carried out by full-matrix least-squares techniques using *SHELXL-97* [40].The crystal data of (**1**-**4**, **7**) and refinement values are summarized in Supplementary Table 1.

Docking protocols

Gold was used to carry out molecular docking. Parameters were used using default settings and keeping receptor rigid. Active site residue His322 for 1e9y and Met762 was selected for 4fm9 around which a grid of 10 Å was defined as binding site. Gold Score fitness function, assigned to each docked ligand was used to assess the results. Binding affinities of the used compounds were then calculated using AutoDock\Vina. Grid spacing of 1.0 Å was used with a box size of 10×10×10 with xyz coordinates of active site centre. Best ligand was selected on the bases of Gold Score and Binding energy values.

Structure selection and preparation

For molecular docking studies, structures were extracted from PDB data base having PDB:IDs (1e9y) and (4fm9). These structures were then minimized using Chimera 1.8.1.

Docking studies

GOLD (Genetic Optimization for Ligand Docking) was used for molecular docking studies [41]. This software utilizes a genetic algorithm for docking flexible ligands into protein binding sites to explore the full range of ligand conformational flexibility with partial protein

View Article Online
DOI: 10.1039/C6RA19162B

flexibility [42]. The binding site definition should therefore be large enough to contain any possible binding mode of the ligand. In this work we specified the approximate centre of the binding site and atoms that lie within a specified radius of 10 A°. The standard default settings such as population size (100), selection pressure (1.1), niche size(2), and operator weights for migrate (0), crossover (100), number of operations (10,000), number of islands (1) and number of dockings 10 were adapted for docking process. These calculations were performed with GOLD5.1 on Intel Xeon QuadTM Core processor 3.0 GHz Linux workstation running under open SUSE11.3.

Molecular Dynamic Simulation

Docked complex of compound **3** with 1E9Y and 4FM9 were simulated to obtained their detailed mechanistic and dynamics with respect to their targets. AMBER 14 simulation package was utilized [43]. Antechamber program was used to generate initial library and parameters for compound **3** and a non-standard residue KCX carbamylated lysine in 1E9Y. Leap program helped in integration of docked complex into a TIP3P water box of size 12 Å with ff14SB force field describing the molecular interactions of the system. 10 Na^+ and 5 Cl^-were added to hydrated complexes of 1E9Y and 4FM9 respectively to neutralize the system. The system energy were minimized gradually, first the Hydrogen of the entire system were relax with 500 cycle of minimization; followed by minimization of water box with cycles of 1000 with a restraint of 200 kcal/mol –$Å^2$. After that the system was minimized with 1000 cycles and a restraint of 5 kcal/mol –$Å^2$ on carbon alpha atoms. Then all non-heavy atoms were minimized using 300 cycles and restraint of 100 kcal/mol –$Å^2$. After performing minimization, system was heated to 300 K for 20 picoseconds (ps) with a time step of 2 femtoseconds (fs) and 5 kcal/mol –$Å^2$ restraint on carbon alpha atoms. Temperature was maintained using langevin dynamics with gamma ln value set to 1.0. SHAKE was applied for constraining bonds with hydrogen and NVT ensemble was selected for heating the systems. The molecule was then equilibrated for 100 ps with 2 fs time step, with SHAKE applied on hydrogen bonds and langevin dynamics for temperature scaling [44]. NPT ensemble was utilized with isotropic position scaling to maintain pressure. Carbon alpha positions were restrained by 5 kcal/mol –$Å^2$. Same set of parameters were used for another 50 ps, with an exception of reducing the restraint on carbon after every 10 ps by 1kcal/mol –$Å^2$. The system was then allowed to equilibrate itself under same set of condition for 1 ns. For production NVT ensemble was selected with Berendsen temperature coupling algorithm [45]. SHAKE was applied on hydrogen bonds and cut off value for non-bonded interaction was set to 8.0 Å. The production run was carried out for 50 ns on a time step of 2 fs. The simulation trajectories were analysed using ccptraj program of AMBER package and structural parameters like RMSD and RMSF were calculated. The trajectory were visually analysed using VMD [38] and Chimera [46]. There depictions were captured using these tools.

Conclusions

In conclusion, we have developed an efficient and convenient Ph_3GeH-catalyzed one-pot reaction from 4-methylpent-3-en-2-one (**I**) and thioureas **II**(**a**-**h**) obtained from readily available substituted anilines for the synthesis of a series of substituted dihydropyrimidine derivatives. It is interesting that the addition of thiourea to 4-methylpent-3-en-2-one (**I**) as final step towards product formation successfully explains the debate about addition of thiourea to aldehyde or to ethyl acetoacetate as first step in Biginelli dihydropyrimidine synthesis. Hence not only simplicity of this Biginelli's one-pot combination is preserved here but also consistent production of excellent yields of the dihydropyrimidin-2(*1H*)-thione is also achieved along with higher functional groups tolerance. By further elaboration and diversification of the various functional groups, a wide range of *N*-heterocycles can be produced. The Ph_3GeH-catalyzed one-pot process may find potential applications in the synthesis of biologically and medicinally relevant compounds in future research endeavours. *In silico* studies were carried out to find the binding pattern of urease inhibitors. Furthermore, the results suggest that these derivatives may be used as preventive/ chemotherapeutic agents for cancer. Hence it is

View Article Online
DOI: 10.1039/C6RA19162B

recommended to find their role as urease inhibitors and anticancer agents by applying *in vitro* and *in vivo* studies to find some meaningful conclusions.

Acknowledgements

The authors are thankful to Quaid-i-Azam University and Higher Education Commission of Pakistan, Islamabad, Pakistan for the grant of funds for this project.

Notes and references

1 P. Salehi, M.Dabiri, M. A. Zolfigol and M. A. B. Fard, *Tetrahedron Lett.,* 2003, **44**(14), 2889-2891.

2 V. S. Dinakaran, D. Jacob, J. E. Mathew, *Med. Chem. Res.,* 2012, **21**(11), 3598-3606.

3 C. O. Kappe, *Eur. J. M. Chem.,* 2000, **35**(12), 1043-1052.

4 M. Nasr-Esfahani and A. R. Khosropour, *Bull. Korean Chem. Soc.,* 2005, **26**(9), 1331.

5 G. Senthilkumar. PhD Thesis (Green synthesis, characterization and biological studies of some novel organofluoro compounds). Annamalai University, India. 2015.

6 K. S. Atwal, G. C. Rovnyak, J. Schwartz, S. Moreland, A. Hedberg, J. Z. Gougoutas, M. F. Malley and D. M. Floyd, *J. Med. Chem.,* 1990, **33**(5), 1510-1515.

7 M. G. Kulkarni, S. W. Chavhan, M. P. Shinde, D. D. Gaikwad, A. S. Borhade, A. P. Dhondge, Y. B. Shaikh, V. B. Ningdale, M. P. Desaiand and D. R. Birhade, *Beilstein J. Org. Chem.,* 2009, **5**(1), 4.

8 C. O. Kappe, *J. Org. Chem.,* 1997, **62**(21), 7201-7204.

9 M. Matache, C. Dobrota, N.D. Bogdan and D.P. Funeriu, *Curr. Org. Synth.,* 2011, **8**(3), 356-373.

10 A. Debache, M. Amimour, A. Belfaitah, S. Rhouati and B. Carboni, *Tetrahedron Lett*., 2008, **49**, 6119–6121.

11 C. V. Reddy, M. Mahesh, P. Raju, T. R. Babu and V. N. Reddy, *Tetrahedron Lett.,* 2002, **43**(14), 2657-2659.

12 (a) A. Elmaghraby, I. Mousa, A. Harb and M. Mahgoub, ISRN Organic Chemistry, 2013. (b) N.-Y. Fu, Y.-F. Yuan, Z. Cao, S.-W. Wang, J.-T. Wang, and C. Peppe, *Tetrahedron*, 2002, **58**(24), 4801–4807.

13 M.A. Bigdeli, S. Jafari, G. H. Mahdavinia and H. Hazarkhani, *Catalysis Communications*, 2007, **8**, 1641–1644.

14 C.-J. Liu and J.-D. Wang, *Molecules,* 2009, **14**, 763–770.

15 H. X. Lin, Q. J. Zhao, B. Xu and X. H. Wang, *Chin. Chem. Lett.,* 2007, **18**, 502–504.

16 D. L. da Silva, S. A. Fernandes, A. A. Sabino, A. de Fatima, *Tetrahedron Lett.,* 2011, **52**, 6328–6330.

17 (a) M. Litvic´, I. Vecenaj, Z. M. Ladisic´, M. Lovric´, V. Vinkovic´ and M. F-Litvic´, *Tetrahedron,* 2010, **6** 3463-3471. (b) S. Ramalingam and P. Kumar, *Synth. Commun.,* 2009, **39**, 1299-1309. (c) S. L. Jain, J. K. Joseph, S. Singhal and B. Sain, *J. Mol. Catal. A: Chem.*, 2007, **268**, 134-138. (d) J. Lu, Y. Bai, Z. Wang, B. Yang and H. Ma, *Tetrahedron Lett*., 2000, **41**, 9075–9078. (e) A. Debache, B. Boumoud, M. Amimour, A. Belfaitah, S. Rhouati and B. Carboni, *Tetrahedron Lett*., 2006, **47**, 5697–5699

18 Imtiaz-ud-Din, K. C. Molloy, M. Mazhar, S. Dastgir, S. Ali and M. F. Mahon, *Appl .Organometal. Chem.,* 2003, **17**(10), 781-787.

19 Imtiaz-ud-Din, M. Mazhar, S. Dastgir, M. F. Mahon and K. C. Molloy, *Appl. Organometal. Chem.,* 2003, **17**(10), 801-802.

20 Imtiaz-ud-Din, M. Mazhar, K. M. Khan, M. F. Mahon and K. C. Molloy, *J. Organomet. Chem.,* 2004, **689**(5), 899-908.

21 H. G. O. Alvim, T. B. Lima, A. L. de Oliveira, H. C. B. de Oliveira, F. M. Silva, F. C. Gozzo, R. Y. Souza, W. A. da Silva and B. A. D. Neto, *J. Org. Chem.,* 2014, **79**, 3383−3397.

22 (a) F. G. Klein and J. T. Banchero, *Ind. Eng. Chem*., 1956, **48**(8), 1276-1286. (b) J. H. Clark, D. J. Macquarrie, and J. Sherwood, *Chem. Eur. J.*, 2013, **19**, 5174 – 5182.

23 M. Rubin, T. Schwier and V. Gevorgyan, *J. Org. Chem*., 2002, **67**(6), 1936-1940.

24 Imtiaz-ud-Din, M. Mazhar and K. C. Molloy, *Main Group Metal Chemistry*, 2006, **29**(1), 11-20.

25 Imtiaz-ud-Din, M. Mazhar, K. Molloy and K. M. Khan, *J. Organomet. Chem., 2006*, **691**(8), 1643-1648.

View Article Online
DOI: 10.1039/C6RA19162B

26 S. Schweizer, C. Tresse, P. Bisseret, J. Lalevée, G. Evano and N. Blanchard, *Org. Lett.,* 2015, **17**(7), 1794-1797.
27 K. Miura, Y. Ichinose, K. Nozaki, K. Fugami, K. Oshima and K. Utimoto, *Bull. Chem. Soc. Jpn.,* 1989, **62**(1), 143-147.
28 T. Matsuda, S. Kadowaki, Y. Yamaguchi and M. Murakami, *Chem. Comm.,* 2008, **24**, 2744-2746.
29 F. Wada, S. Abe, N. Yonemaru, K. Kikukawa and T. Matsuda, *Bull. Chem. Soc. Jpn.,* 991, **64**(5), 1701-1703.
30 Y. Ichinose, H. Oda, K. Oshima and K. Utimoto, *Bull. Chem. Soc. Jpn.,* 1987, **60**(9), 3468-3470.
31 T. Matsuda, S. Kadowaki, Y. Yamaguchi and M. Murakami, *Org. Lett*., 2010, **12**(5), 1056-1058.
32 R. N. Naumov, M. Itazaki, M. Kamitani and H. Nakazawa, *J. Am. Chem. Soc.,* 2012, **134**(2), 804-807.
33 (a) T. Schwier and V. Gevorgyan, *Org. Lett*., 2005, **7**(23), 5191-5194. (b) S. Schweizer, C. Tresse, P. Bisseret, J. Laleve, G. Evano and N. Blanchard, *Org. Lett.,* 2015, **17**, 1794–1797.
34 V. Tamaddon, Z. Razmi and A.A. Jafari, *Tetrahedron Lett.*, 2010, **51**, 1187–1189.
35 A. Sharma, R. Khare, V. Kumar, G. K. Gupta and V. Beniwal, *Int. J. Pharm. Pharm. Sci.,* 2014, **6**(3), 171-175.
36 H. O. Kalinowski, S. Berger and S. Brown, Thieme, Verlag, Stuttgart, Germany, 1984, **218**.
37 W. Humphrey, A. Dalke and K. Schulten. *J. Molec. Graphics*, 1996, **14.1**, 33-38.
38 A. C. Wallace, R. A. Laskowski and J. M. Thornton. *Protein Eng.*, 1996, **8**, 127-134.
39 G. M. Sheldrick, *Acta Crystallogr. Sect. A*, 2008, **64**, 112–122.
40 G. Jones, P. Willett and R. C. Glen. *J. Mol. Biol.,* 1995, **245**, 43–53.
41 G. Jones, P. Willett, R. C. Glen, A. R. Leach and R. Taylor, *J. Mol. Biol.,* 1997, **267**, 727–748.
42 D.A. Case, V. Babin, J.T. Berryman, R.M. Betz, Q. Cai, D.S. Cerutti, T.E. Cheatham, III, T.A. Darden, R.E. Duke, H. Gohlke, A.W. Goetz, S. Gusarov, N. Homeyer, P. Janowski, J. Kaus, I. Kolossváry, A. Kovalenko, T.S. Lee, S. LeGrand, T. Luchko, R. Luo, B. Madej, K.M. Merz, F. Paesani, D.R. Roe, A. Roitberg, C. Sagui, R. Salomon-Ferrer, G. Seabra, C.L. Simmerling, W. Smith, J. Swails, R.C. Walker, J. Wang, R.M. Wolf, X. Wu and P.A. Kollman, 2014, AMBER **14**, University of California, San Francisco.
43 J. P. Ryckaert, G. Ciccotti and H. J. Berendsen, *J. Comput. Phys.,* 1977, **23**, 327-341.
44 H. C. Andersen, *J. Chem. Phys.,* 1980, **72**, 2384-2393.
45 E. F. Pettersen, T. D. Goddard, C. C. Huang, G. S. Couch, D. M. Greenblatt, E. C. Meng and T. E. Ferrin, *J. Comput. Chem.,* 2004, **25**, 1605-1612.

View Article Online
DOI: 10.1039/C6RA19162B

Graphical Abstract

A series of substituted dihydropyrimidin-2(*1H*)-thione derivatives (**1**-**8**) have been synthesized and docked against enzymes Human topoisomerase II alpha (4fm9) and Helicobacter pylori Urease (1E9Y) for binding modes validation.